

FIG. 3. Spatial distribution of 29-cm^{-1} phonons in the crystal 200 nsec after emission of the heat pulse. The width of the ballistic phonon pulse in (a) is larger than the 0.6 mm expected from the duration of the heat pulse (100 nsec) due to the dimension of the detector volume [$d_x = 1$ mm in Fig. 1(b)]. The curve in (b) indicates the imprisonment of 29-cm^{-1} phonons directly behind the heater when the crystal contains a larger concentration of excited Cr^{3+} .

in the crystal as phonons, in contrast to the systems studied up to now for which trapped resonant radiation is stored mainly as electronic excitation energy (in case of trapped bottleneck phonons^{6,7} as well as in case of trapped resonant photons^{8,9}).

Therefore, we can determine the lifetime τ_{ph} of the 10^{12} -Hz phonons from the exponential decay of the imprisoned phonons [Fig. 2(b)]. The resulting time, $\tau_{ph} \approx 1.5 \mu\text{sec}$, corresponds to the spontaneous decay time of the 29-cm^{-1} phonons in ruby because no temperature dependence between 4.2 and 2°K has been observed.

Applications of the described detection principle for 10^{12} -Hz phonons are in preparation for other crystal-impurity systems. By applying external fields to the crystal it should be possible to realize tunable detectors for 10^{12} -Hz phonons, thus extending the region of existing phonon spectrometers.¹⁰

The authors would like to thank K. Dransfeld and C. Kittel for very stimulating discussions. We acknowledge conversations with G. Nath and experimental assistance by J. Peckenzell.

¹S. Geschwind, G. E. Devlin, R. L. Cohen, and S. R. Chinn, *Phys. Rev.* **137**, A1087 (1965).

²M. Blume, R. Orbach, A. Kiel, and S. Geschwind, *Phys. Rev.* **139**, A314 (1965).

³R. J. von Gutfeld and A. H. Nethercot, *Phys. Rev. Lett.* **12**, 641 (1964).

⁴O. Weis, *Z. Angew. Phys.* **26**, 325 (1969).

⁵A. Morton, *Appl. Opt.* **7**, 1 (1968).

⁶J. A. Giordmaine and F. R. Nash, *Phys. Rev.* **138**, A1510 (1965).

⁷*Spin-Lattice Relaxation in Ionic Solids*, edited by A. A. Manenkov and R. Orbach (Harper and Row, New York, 1966).

⁸M. Zemansky, *Phys. Rev.* **29**, 513 (1927).

⁹T. Holstein, *Phys. Rev.* **72**, 1212 (1947).

¹⁰C. H. Anderson and E. S. Sabisky, *Phys. Rev. Lett.* **21**, 987 (1968).

Observation of Simultaneous Excitation of the Coupled Cr^{3+} Ions to the 2E_g States in $\text{LaAlO}_3:\text{Cr}^{3+}$

J. P. van der Ziel

Bell Telephone Laboratories, Murray Hill, New Jersey 07974

(Received 1 February 1971)

Transitions to the states of Cr^{3+} pairs where both ions are excited to the 2E_g levels have been observed in $\text{LaAlO}_3:\text{Cr}^{3+}$. Of the predicted eight pair levels, three of the $S=0$ and one of the $S=1$ levels have definitely been identified at approximately twice the 2E_g energy absorption. The remaining transitions either are obscured by the strong vibronic spectrum or are very weak. The polarization of the lines agrees with a model based on the mechanism of exchange-induced electric dipole moment.

Previous studies of exchange-coupled Cr^{3+} pairs have been concerned with the spectra resulting from transitions between the pair levels where both ions are in the 4A_2 ground state and levels where one of the ions is in the 2E state and

the other in the 4A_2 state.¹ We report the experimental observation of a sharp line spectrum of Cr^{3+} pairs in LaAlO_3 resulting from transitions to levels where both ions of the pair are in the 2E_g state. The levels are found at approximately

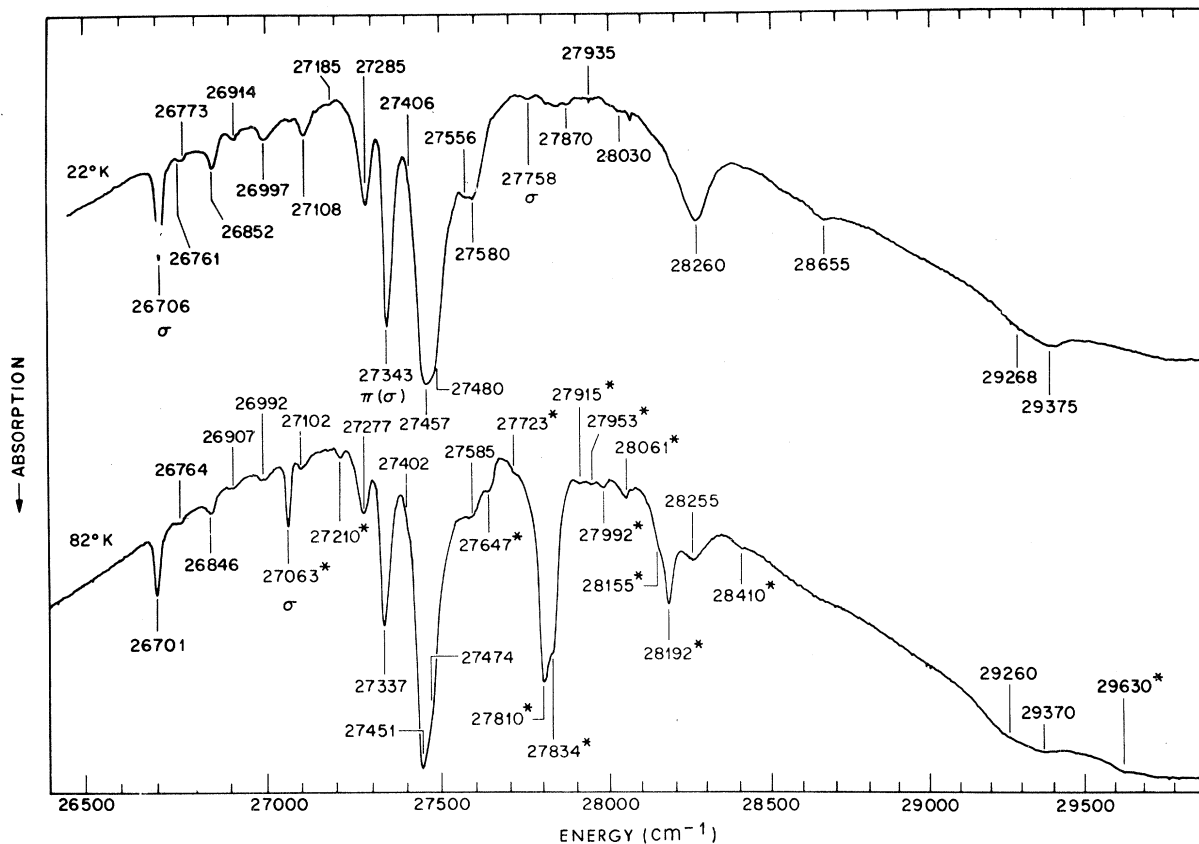


FIG. 1. Absorption spectrum of Cr^{3+} pairs in LaAlO_3 resulting from the excitation of both Cr^{3+} ions to the 2E_g state. The lines with a definite polarization are denoted by σ or π . The low-temperature transitions originate on the $S=0$ ground-state pair level, and the additional high-temperature transitions (*) on the $S=1$ level.

twice the 2E_g energy.

The uv absorption spectra at 22 and 82°K are shown in Fig. 1. Monochromatic radiation from a 1-m Czerny-Turner spectrometer equipped with a 200-W tungsten lamp and appropriate filters was incident on a crystal which was held in a variable-temperature Dewar. The transmitted radiation was detected by an S-20 response photomultiplier equipped with a uv-transmitting filter. In order to show adequate detail, the zero-transmission base line is off scale. The crystal nominally contained about 1.0 wt% Cr^{3+} .

These lines appear as a broad band in the low-resolution pair excitation spectrum of the near-infrared spectrum of Tkachuk and Zonn.² The band was identified as an excited state of the pair from (a) the nonlinear concentration dependence, (b) the enhancement in the pair emission relative to the single-ion emission as compared to the intensities when the ${}^4T_{1g}$ or ${}^4T_{2g}$ single-ion bands are excited, and (c) the time dependence of the emission following pulsed excitation.² The excitation spectrum has been re-examined using a

detector sensitive either to the single-ion R -line emission or to the strongest pair line at $13\,368.5\text{ cm}^{-1}$. At low temperatures the uv lines are not present when the R -line emission is monitored, thus eliminating the possibility that these are transitions to higher-energy doublet levels. Such transitions have recently been observed in the excited-state absorption spectrum of ruby.³ Linz and Newnham have reported a complex structure at approximately twice the R -line energy in ruby.⁴ These transitions were also attributed by them to higher energy doublets with the nonlinear concentration dependence arising from an exchange enhancement of the transitions in the pair system. A similar enhancement is expected for the pair transitions involving the 2E_g level. Indeed these lines are found in LaAlO_3 to have electric-dipole polarization (the R lines are magnetic dipole), and to have the selection rule $\Delta S=0$ and for the strongest lines $\Delta M_s=0$, indicating that the strength of the pair emission comes mainly from the mechanism of exchange-induced electric dipole moment.^{5,6} However, for mea-

measurements made on a 0.05% sample, and at $T > 100^\circ\text{K}$ where the excited-pair levels are populated, the infrared pair absorption was at most 0.3 times the R -line absorption. Even if the exchange of the uv dipole moments is a factor of 10 larger than that for the infrared pair lines, the single-ion transitions should have been easily observed in the excitation spectrum, thus ruling out the possibility that in our material the strongest uv lines result from the mechanism described by Linz and Newnham.

The splittings of the ground-state pair levels are given by

$$E(\vec{S}) = -J^{ab} \vec{S}^a \cdot \vec{S}^b, \quad (1)$$

where \vec{S}^a , \vec{S}^b are the spins of the two ions. The ground-state single-ion levels of an antiferromagnetic pair combine to form a lowest energy level with $S = |\vec{S}^a + \vec{S}^b| = 0$, and levels with $S = 1, 2$, and 3 at energies $-\frac{1}{2}J^{ab}S(S+1)$. From infrared absorption and emission measurements we obtain $J^{ab} = -67.6 \text{ cm}^{-1}$ for the nearest-neighbor exchange. This differs from the published values of $J^{ab} = -39.8 \pm 1 \text{ cm}^{-1}$ of Blazey and Burns⁷ and -98 cm^{-1} of Tkachuk and Zonn.²

The near-infrared levels of the pair are formed from the coupling of the 2E_g and ${}^4A_{2g}$ states of the pair to yield four pair states with $S=1$ and four with $S=2$. The exchange splittings of the excited state are derived from the more general form

$$\mathcal{H}_{ex}^{ab} = -\sum_{i,j} J_{ij} \vec{s}_i^a \cdot \vec{s}_j^b, \quad (2)$$

where \vec{s}_i^a and \vec{s}_j^b are the spins of the t_{2g} electrons of ions a and b , respectively, and J_{ij} is a function of the orbitals.^{8,9}

The pair levels corresponding to both ions in the 2E_g states consist of four states with $S=0$, $M_s=0$, and four states with $S=1$, $M_s=0, \pm 1$. Since the 2E_g levels are involved, the exchange splittings are obtained from Eq. (2) rather than from Eq. (1).

The temperature dependence of the absorption enables us to identify the ground-state pair levels involved in the transitions. With increasing temperature the absorption coefficients of the low-temperature lines decrease uniformly, and a new spectrum appears with increasing intensity. The latter are denoted in Fig. 1 by an asterisk. Figure 2 is a plot of the T^{-1} dependence of the 26701- and 27810- cm^{-1} absorption coefficients which are typical of the two groups. The coefficients have been plotted on a relative vertical scale to

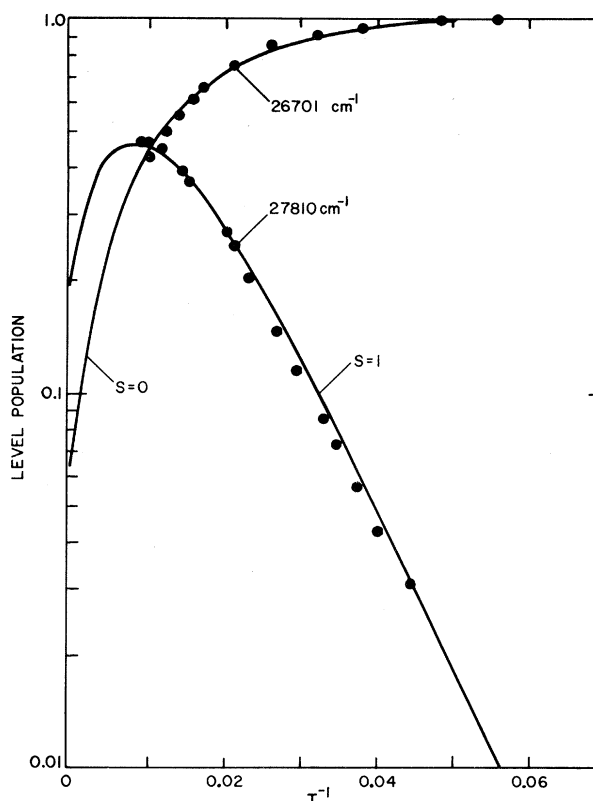


FIG. 2. Curves: the populations of the $S=0$ and 1 ground-state pair levels as a function of T^{-1} . Solid points: the measured absorption coefficients of the 26701- and 27810- cm^{-1} lines multiplied by a constant factor.

bring the points into coincidence with the calculated probabilities for a nearest-neighbor pair to be in the $S=0$ and 1 ground-state levels, which are given by

$$P(S) = (2S+1) \exp\left(-\frac{E(S)}{kT}\right) \times \left[\sum_{S'=0}^3 (2S'+1) \exp\left(-\frac{E(S')}{kT}\right) \right]^{-1} \quad (3)$$

where the ground-state splittings $E(S)$ are given by Eq. (1).

The two types of absorption are identified with $S=0 \rightarrow 0$ and $S=1 \rightarrow 1$ transitions, respectively, the transitions with $\Delta S = \pm 1$ and ± 2 being negligibly weak. This selection rule, and the predominant electric-dipole polarization of several of the lines, indicates the double excitation gains its intensity from the mechanism of exchange-induced electric dipole moment. Figure 2 provides additional confirmation that the higher-energy exchange-coupled doublets are not involved. These levels have $S=1$ and 2, and the $\Delta S=0$ selection rule predicts that the strongest absorption would

occur from the $S=1$ and 2 levels.

The uv levels, together with the levels of the singly excited pair, and the ground-state levels should provide a good test of the excited-state exchange-interaction theories.^{6,8,9} Because of its relatively simple structure the LaAlO_3 host is especially suitable for such a comparison. As indicated above, only first nearest-neighbor exchange is important. Furthermore, the coupling proceeds via an approximately collinear bond (the actual $\text{Al}^{3+}-\text{O}^{2-}-\text{Al}^{3+}$ angle of the host is¹⁰ 166.8°). The exchange splittings have been calculated from Eq. (2) for the C_2 symmetry of the nearest-neighbor pair in terms of the empirical parameters J_{ij} .⁶ The exchange-induced shifts of the $S=1$ level are found to be just $-\frac{1}{3}$ the shifts of the $S=0$ levels. The polarization of the lines has also been calculated using the mechanism of exchange-induced dipole moment:

$$\vec{P} = \sum_{i,j=1}^3 \vec{P}_{ij}(\vec{s}_i \cdot \vec{s}_j), \quad (4)$$

where the \vec{P}_{ij} are empirical parameters. The matrix elements of Eq. (4) were evaluated using the wave functions which diagonalize Eq. (2). Transitions to two of the $S=0$ as well as the $S=1$ levels are predicted to be relatively strong and appear in σ and α polarization. Experimentally these transitions are found at 26 701 and 27 758 cm^{-1} for $S=0$, and at 27 063 cm^{-1} for $S=1$. The remaining σ - and α -polarized $S=1$ transition has not been identified. For both S values the theory further predicts a third transition to be strong in all polarizations, while the transitions to the remaining levels are significantly weaker. A comparison with the theory and the experimental results of the infrared pair spectrum shows that these uv transitions are expected to be strongest in π polarization. Since the strong $S=0$ line at 27 337 cm^{-1} has this polarization, it is identified with this transition. We have thus identified four of the predicted six strong transitions. The energy level diagram is shown in Fig. 3. A striking feature of Fig. 1 is the vibronic spectrum associated with the lowest-energy σ -polarized lines which severely complicates the finding of the remaining transitions. The strong vibronics of the doubly excited states indicate that these levels are a sensitive function of the crystal field, and that the displacement of the energy parabolas on the configuration-coordinate diagram is considerably larger than the displacement for the singly excited states.¹¹ The σ -polarized transitions terminate on pair levels having *both* ions in ei-

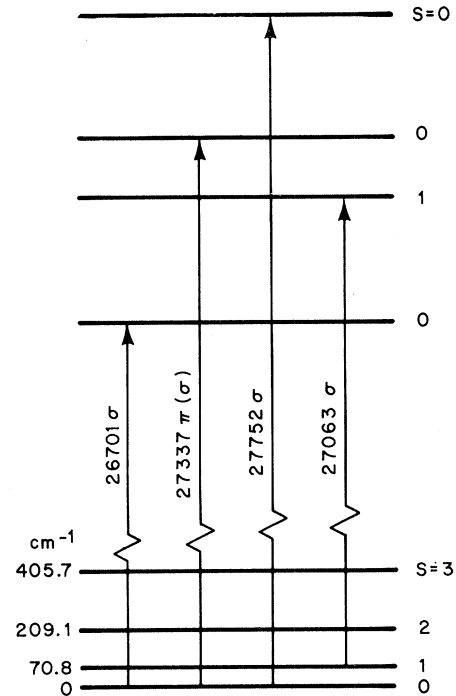


FIG. 3. Energy levels of the nearest neighbors. The transitions to the states with both ions in the 2E levels are shown.

ther the ${}^2E_\epsilon$ or ${}^2E_\theta$ states. For these levels, symmetry arguments show that the spin-dependent dipole moment vanishes in the cubic perovskite phase.⁶ Its existence in the low-temperature rhombohedral phase is due to the lowering of the symmetry resulting from a distortion of the O^{2-} ions from their cubic positions. Raman-scattering experiments show that the soft modes associated with the phase transition are at 40 cm^{-1} (A_{1g}) and 147 cm^{-1} (E_g) at low temperatures.¹² Because the symmetries are the same, the E_g phonon will couple most strongly to the electronic excited states. The vibronics of both σ -polarized transitions are indeed mainly well-defined multiples of this mode.

The terminal states of the infrared pair absorption involve one ion in the 4A_2 state and the other in a 2E state. The 27 343- cm^{-1} transition results in one ion in each of the ${}^2E_\theta$ and ${}^2E_\epsilon$ states. These transitions consequently do not have strong vibronic sidebands.

A comparison of the exchange splittings of the ground states, the singly excited states, and the doubly excited states shows that the exchange splittings and the J_{ij} parameter increase with increasing energy.⁶ This implies that the overlap of the Cr^{3+} wave functions with the O^{2-} ligand is larger in the 2E states than in the 4A_2 state.

¹The energy levels of Cr^{3+} pairs in ruby have recently been discussed by P. Kisliuk, N. C. Chang, P. L. Scott, and M. H. L. Pryce, *Phys. Rev.* **184**, 367 (1969).

²A. M. Tkachuk and Z. N. Zonn, *Opt. Spektrosk.* **26**, 587 (1969) [*Opt. Spectrosc.* **26**, 322 (1969)].

³T. M. Dunn and A. H. Francis, *Phys. Rev. Lett.* **25**, 705 (1970).

⁴A. Linz, Jr., and R. E. Newnham, *Phys. Rev.* **123**, 500 (1961).

⁵Y. Tanabe, T. Moriya, and S. Sugano, *Phys. Rev. Lett.* **15**, 1023 (1965). See also R. Loudon, *Advan. Phys.* **17**, 243 (1968).

⁶J. P. van der Ziel, to be published.

⁷K. W. Blazey and G. Burns, *Phys. Lett.* **15**, 117 (1965).

⁸N. L. Huang, *Phys. Rev. B* **1**, 945 (1970).

⁹M. H. L. Pryce, unpublished.

¹⁰M. Marezio, J. P. Remeika, and P. D. Dernier, unpublished. I am indebted to these authors for the use of their crystallographic x-ray prior to publication.

¹¹C. C. Klick and J. H. Schulman, in *Solid State Physics*, edited by H. Ehrenreich, F. Seitz, and D. Turnbull (Academic, New York, 1957), Vol. 5, p. 97.

¹²J. F. Scott, *Phys. Rev.* **183**, 823 (1969).

Normal Modes of Vibrations in CuCl

C. Carabatos,* B. Hennion, K. Kunc,† F. Moussa, and C. Schwab*

Centre d'Etudes Nucléaires de Saclay, Saclay, France

(Received 23 November 1970)

The frequency-wave-vector dispersion relation $\nu(\vec{q})$ for the normal vibrations of a CuCl single crystal at room temperature has been measured for the [100]-, [110]-, and [111]-symmetric directions using inelastic neutron scattering.

In view of the interest in studying the lattice dynamics of crystals with zinc-blende structure, we present in this paper the results of coherent inelastic neutron scattering on cuprous chloride (CuCl). Our particular attention was drawn by this material because of its peculiar behavior relative to other crystals with the same symmetry, as pointed out by Martin.¹

The present experiments were performed by means of the triple-axis crystal spectrometer at

the EL3 reactor, Saclay. A collimated beam of monochromatic neutrons, produced by Bragg reflection from a germanium single crystal, was incident upon the CuCl specimen. The energies of the scattered neutrons were determined by Bragg reflection from a second germanium single crystal. The experiments were carried out by using either constant- Q or constant- ν techniques, for waves propagating along the high-symmetry directions [100], [110], and [111].

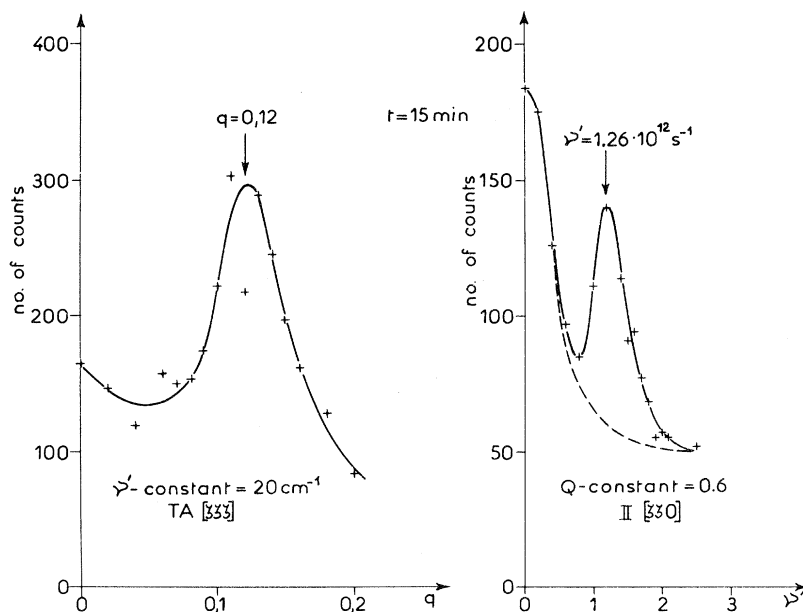


FIG. 1. Typical neutron groups obtained on a CuCl single crystal.